Electronic supplementary information

Metal-organic frameworks based on polynuclear lanthanide complexes and octahedral rhenium clusters

Yulia M. Litvinova,[a] Yakov M. Gayfulin,*[a] Jan van Leusen,[b] Denis G. Samsonenko,[a,c] Vladimir A. Lazarenko,[d] Yan V. Zubavichus,[e] Paul Kögerler[b] and Yuri V. Mironov[a,c]

[a] *Nikolaev Institute of Inorganic Chemistry SB RAS, Acad. Lavrentiev ave. 3, 630090 Novosibirsk, Russia*
E-mail: gayfulin@niic.nsc.ru
[b] *Institute of Inorganic Chemistry, RWTH Aachen University, Landoltweg 1, 52074 Aachen, Germany*
[c] *Novosibirsk State University, Pirogova str. 2, 630090 Novosibirsk, Russia*
[d] *National Research Center "Kurchatov Institute", Kurchatov Square 1, 123182 Moscow, Russia*
[e] *Federal Research Center Boreskov Institute of Catalysis, Lavrentiev Ave. 5, 630090 Novosibirsk, Russia*

Table of contents:

Table 1. Crystallographic data and structure refinement details for compounds **1–9**

	1	**2**	**3**
Empirical formula	$C_{30}H_{44}N_{10}O_{24}Pr_4Re_6S_8$	$C_{33}H_{42}N_{11}Nd_4O_{22}Re_6S_8$	$C_{30}H_{44}N_{10}O_{24}Re_6S_8Sm_4$
M / g mol^{-1}	2866.07	2895.41	2903.83
T / K	130(2)	130(2)	130(2)
Radiation type	Mo K_α	Mo K_α	Mo K_α
Radiation wavelength / Å	0.71073	0.71073	0.71073
Crystal system	Monoclinic	Monoclinic	Monoclinic
Space group	$P2_1/n$	$P2_1/n$	$P2_1/n$
T_{min}, T_{max}	0.586, 1.000	0.581, 1.000	0.191, 1.000
a / Å	22.7792(7)	22.8344(4)	22.7540(4)
b / Å	12.6008(3)	12.5424(2)	12.5264(2)
c / Å	23.8919(7)	23.8734(4)	23.7189(4)
β / °	111.325(3)	111.117(2)	111.036(2)
V / Å^3	6388.3(3)	6378.1(2)	6310.0(2)
Z	4	4	4
ρ_{calc} / g cm^{-3}	2.980	3.015	3.057
μ / mm^{-1}	14.640	14.863	15.455
F(000)	5200	5244	5248
Crystal size / mm^3	0.20×0.19×0.17	0.15×0.05×0.03	0.27×0.18×0.08
2θ range for data collection / °	3.303–28.714	3.297–29.084	3.242–28.723
Index ranges	$-27 \le h \le 24$; $-16 \le k \le 16$; $-31 \le l \le 30$	$-30 \le h \le 30$; $-17 \le k \le 13$; $-27 \le l \le 30$	$-29 \le h \le 29$; $-16 \le k \le 16$; $-32 \le l \le 31$
Collected reflections	35925	32942	80812
R_{int}	0.0239	0.0268	0.0380
Observed reflections	14107	14153	15113
Reflections with $I > 2\sigma(I)$	12296	11766	14180
Goodness-of-fit on F^2	1.019	1.019	1.056
Final R indexes [$I > 2\sigma(I)$]	$R_1 = 0.0292$, $wR_2 = 0.0697$	$R_1 = 0.0311$, $wR_2 = 0.0951$	$R_1 = 0.0277$, $wR_2 = 0.0695$
Final R indexes [all data]	$R_1 = 0.0366$, $wR_2 = 0.0721$	$R_1 = 0.0443$, $wR_2 = 0.0688$	$R_1 = 0.0303$, $wR_2 = 0.0707$
Largest diff. peak and hole / eÅ^{-3}	2.33 (0.85 Å from Pr1) –1.94 (0.58 Å from Pr3)	2.50 (1.18 Å from O9W) –2.15 (0.44 Å from ND3)	4.07 (0.78 Å from Sm1) –3.82 (0.64 Å from Sm1)

Table 1. Crystallographic data and structure refinement details for compounds **1–9** (continued)

	4	**5**	**6**
Empirical formula	$C_{30}H_{42}Eu_4N_{10}O_{23}Re_6S_8$	$C_{30}H_{42}Gd_4N_{10}O_{23}Re_6S_8$	$C_{30}H_{44}N_{10}O_{24}Re_6S_8Tb_4$
M / g mol^{-1}	2892.25	2913.41	2938.11
T / K	100(2)	100(2)	130(2)
Radiation type	Synchrotron	Synchrotron	Mo K_α
Radiation wavelength / Å	0.96990	0.96990	0.71073
Crystal system	Monoclinic	Monoclinic	Monoclinic
Space group	$P2_1/n$	$P2_1/n$	$P2_1/n$
T_{min}, T_{max}	0.074, 0.275	0.095, 0.404	0.253, 1.000
a / Å	22.6868(15)	22.6751(9)	22.6022(7)
b / Å	12.4553(11)	12.4275(6)	12.3896(3)
c / Å	23.6524(17)	23.6074(10)	23.5464(7)
β / °	110.984(3)	110.903(3)	110.930(4)
V / Å^3	6240.2(8)	6214.6(5)	6158.7(3)
Z	4	4	4
ρ_{calc} / g cm^{-3}	3.079	3.114	3.169
μ / mm^{-1}	21.733	22.162	16.614
F(000)	5224	5240	5296
Crystal size / mm^3	0.25×0.12×0.08	0.20×0.05×0.05	0.45×0.07×0.07
2θ range for data collection / °	3.248–29.691	2.759–29.693	3.251–28.541
Index ranges	$-28 \le h \le 28$; $-15 \le k \le 15$; $-29 \le l \le 29$	$-27 \le h \le 26$; $-15 \le k \le 15$; $-29 \le l \le 28$	$-26 \le h \le 27$; $-15 \le k \le 16$; $-31 \le l \le 31$
Collected reflections	72220	62471	52272
R_{int}	0.0564	0.0568	0.0293
Observed reflections	12242	12222	14100
Reflections with $I > 2\sigma(I)$	11939	10986	12531
Goodness-of-fit on F^2	1.089	1.013	1.034
Final R indexes [$I > 2\sigma(I)$]	$R_1 = 0.0363$, $wR_2 = 0.0932$	$R_1 = 0.0382$, $wR_2 = 0.0986$	$R_1 = 0.0291$, $wR_2 = 0.0717$
Final R indexes [all data]	$R_1 = 0.0373$, $wR_2 = 0.0940$	$R_1 = 0.0432$, $wR_2 = 0.1011$	$R_1 = 0.0355$, $wR_2 = 0.0743$
Largest diff. peak and hole / eÅ^{-3}	3.80 (0.80 A from Eu1) –3.74 (0.69 A from Eu1)	1.83 (1.32 A from Re1) –2.39 (0.66 A from Gd1)	2.26 (0.80 Å from Re6) –2.06 (0.48 Å from Tb1)

Table 1. Crystallographic data and structure refinement details for compounds **1–9** (continued)

	7	**8**	**9**
Empirical formula	$C_{30}H_{38}Dy_4N_{10}O_{21}Re_6S_8$	$C_{30}H_{42}Ho_4N_{10}O_{23}Re_6S_8$	$C_{30}H_{42}Er_4N_{10}O_{23}Re_6S_8$
M / g mol^{-1}	2898.38	2944.13	2953.45
T / K	130(2)	130(2)	100(2)
Radiation type	Mo K_α	Mo K_α	Synchrotron
Radiation wavelength / Å	0.71073	0.71073	0.96990
Crystal system	Monoclinic	Monoclinic	Monoclinic
Space group	$P2_1/n$	$P2_1/n$	$P2_1/n$
T_{min}, T_{max}	0.348, 1.000	0.418, 1.000	0.196, 0.377
a / Å	22.5236(7)	22.5433(12)	22.459(4)
b / Å	12.3713(3)	12.3603(6)	12.321(2)
c / Å	23.4758(7)	23.5047(13)	23.420(3)
β / °	110.565(3)	110.435(6)	110.270(8)
V / Å^3	6124.6(3)	6137.2(6)	6079.4(17)
Z	4	4	4
ρ_{calc} / g cm^{-3}	3.143	3.186	3.227
μ / mm^{-1}	16.961	17.218	24.228
F(000)	5192	5288	5304
Crystal size / mm^3	0.18×0.09×0.08	0.31×0.19×0.15	0.10×0.05×0.05
2θ range for data collection / °	3.282–25.348	3.225–28.425	3.263–29.692
Index ranges	$-23 \le h \le 27$; $-11 \le k \le 14$; $-28 \le l \le 26$	$-27 \le h \le 27$; $-14 \le k \le 16$; $-31 \le l \le 30$	$-27 \le h \le 27$; $-13 \le k \le 15$; $-27 \le l \le 28$
Collected reflections	33174	34548	39521
R_{int}	0.0336	0.0329	0.0779
Observed reflections	11148	13011	11944
Reflections with $I > 2\sigma(I)$	10148	12006	11255
Goodness-of-fit on F^2	1.262	1.096	1.054
Final R indexes [$I > 2\sigma(I)$]	$R_1 = 0.0610$, $wR_2 = 0.1292$	$R_1 = 0.0341$, $wR_2 = 0.0740$	$R_1 = 0.0413$, $wR_2 = 0.1076$
Final R indexes [all data]	$R_1 = 0.0673$, $wR_2 = 0.1309$	$R_1 = 0.0385$, $wR_2 = 0.0759$	$R_1 = 0.0440$, $wR_2 = 0.1098$
Largest diff. peak and hole / eÅ^{-3}	2.52 (0.15 Å from N1B) –2.89 (0.75 Å from Dy1)	3.45 (0.85 Å from Ho1) –2.33 (0.57 Å from Ho1)	2.31 (0.72 Å from Re6) –2.84 (0.80 Å from Re6)

Table S1. Selected interatomic distances of compounds **1**–**9**, Å

	Range / Average, Å				
	1 (Ln = Pr)	**2** (Ln = Nd)	**3** (Ln = Sm)	**4** (Ln = Eu)	**5** (Ln = Gd)
Ln–Ln	3.7513(5)–4.0479(6) / 3.92(14)	3.7400(5)–4.0490(5) / 3.93(11)	3.7062(4)–3.9955(4) / 3.88(11)	3.6850(6)–3.9622(6) / 3.85(10)	3.6853(6)–3.9310(6) / 3.84(9)
Ln–(μ_3-O)	2.398(5)–2.518(5) / 2.45(4)	2.385(5)–2.533(5) / 2.44(4)	2.365(4)–2.484(4) / 2.41(4)	2.380(6)–2.460(6) / 2.40(4)	2.336(6)–2.433(6) / 2.39(3)
Ln–O_{COO-}	2.390(6)–2.572(6), 2.732(5) / 2.46(8)	2.330(6)–2.561(5), 2.738(5) / 2.44(8)	2.348(5)–2.530(6), 2.767(6) / 2.43(8)	2.336(6)–2.560(10), 2.775(11) / 2.42(8)	2.23(2)–2.55(1), 2.75(1) 2.39(10)
Ln–N_{INA}	2.754(6) (N1A)	2.736(6) (N1A)	2.718(5) (N1A)	2.692(8) (N1A)	2.667(9)
Ln–O_{H2O}	2.49(2)–2.61(1) / 2.53(4)	2.496(5)–2.626(6) / 2.55(6)	2.421(12)–2.594(6) / 2.49(6)	2.413(8)–2.583(11) / 2.48(6)	2.39(2)–2.62(2) / 2.47(8)
Ln–N_{CN}	2.598(6)–2.714(6) / 2.62(6)	2.546(6)–2.672(6) / 2.61(5)	2.520(5)–2.663(5) / 2.58(6)	2.493(7)–2.650(7) / 2.55(6)	2.478(8)–2.635(7) / 2.54(6)
Re–Re	2.5859(4)–2.6071(4) / 2.595(7)	2.5882(4)–2.6107(4) / 2.600(6)	2.5919(3)–2.6109(3) / 2.602(6)	2.5892(5)–2.6117(4) / 2.600(7)	2.5898(5)–2.6114(5) / 2.600(7)
Re–S	2.392(2)–2.410(2) / 2.401(5)	2.399(2)–2.414(2) / 2.405(4)	2.399(1)–2.415(2) / 2.407(4)	2.395(2)–2.411(2) / 2.404(4)	2.395(2)–2.410(2) / 2.403(3)
Re–C_{CN}	2.097(7)–2.127(8) / 2.12(1)	2.082(7)–2.124(8) / 2.11(2)	2.085(6)–2.134(6) / 2.12(2)	2.084(9)–2.141(9) / 2.12(2)	2.103(9)–2.143(10) / 2.12(2)

Table S1. Selected interatomic distances of compounds **1**–**9**, Å (continued)

	Range / Average, Å			
	6 (Ln = Tb)	**7** (Ln = Dy)	**8** (Ln = Ho)	**9** (Ln = Er)
Ln–Ln	3.6876(4)–3.8716(4) / 3.81(7)	3.6876(13)–3.8566(12) / 3.79(6)	3.6911(5)–3.8652(5) / 3.78(7)	3.6693(7)–3.8384(7) / 3.76(7)
Ln–(μ_3-O)	2.331(4)–2.425(5) / 2.37(3)	2.306(13)–2.462(13) / 2.36(4)	2.316(5)–2.449(5) / 2.36(4)	2.303(6)–2.429(6) / 2.35(4)
Ln–O_{COO-}	2.28(1)–2.48(2) / 2.35(3)	2.18(5)–2.36(1) / 2.30(4)	2.273(5)–2.356(6) / 2.30(3)	2.268(7)–2.338(6) / 2.29(3)
Ln–N_{INA}	2.604(7) (N1A)	2.60(2) (N1A) 2.53(2) (N1B)	2.584(8) (N1A) 2.558(7) (N1B)	2.576(8) (N1A) 2.572(8) (N1B)
Ln–O_{H2O}	2.354(14)–2.481(6) / 2.42(5)	2.38(2)–2.43(2) / 2.40(2)	2.369(6)–2.437(7) / 2.40(3)	2.341(6)–2.416(8) / 2.38(3)
Ln–N_{CN}	2.477(6)–2.629(6) / 2.54(6)	2.47(2)–2.59(2) / 2.53(5)	2.474(7)–2.583(8) / 2.53(5)	2.430(8)–2.568(9) / 2.51(5)
Re–Re	2.5895(4)–2.6112(3) / 2.599(7)	2.5905(11)–2.6064(10) / 2.598(6)	2.5971(5)–2.6152(4) / 2.606(6)	2.5960(6)–2.6136(6) / 2.604(6)
Re–S	2.395(2)–2.410(2) 2.404(4)	2.394(5)–2.415(5) / 2.403(5)	2.398(2)–2.421(2) / 2.409(6)	2.397(2)–2.420(2) / 2.407(5)
Re–C_{CN}	2.081(7)–2.137(7) 2.12(2)	2.10(2)–2.13(2) / 2.11(1)	2.113(8)–2.137(8) 2.123(9)	2.122(10)–2.160(9) / 2.13(1)

Table S2. Coordination environment and coordination number of lanthanide ions in compounds **1–9**

Compound	Atom	Coordination number	O(H_2O)	O(COO, *ina*)	μ_3-O	N(CN)	N(*ina*)
1–4	Ln1	9	1	2	3	2	1
	Ln2	9	1	3	3	2	–
	Ln3	8	2	2	3	1	–
	Ln4	8	2	2	3	1	–
5	Gd1	8 / 9	– / 1	2	3	2	1
	Gd2	8 / 9	1	2 / 3	3	2	–
	Gd3	8	2	2	3	1	–
	Gd4	8	2	2	3	1	–
6	Tb1	8	– / 1	2 / 1	3	2	1
	Tb2	8	1	2	3	2	–
	Tb3	8	2	2	3	1	–
	Tb4	8	2	2	3	1	–
7	Dy1	8	–	2	3	2	1
	Dy2	8	1 / –	2	3	2	– / 1
	Dy3	8	2	2	3	1	–
	Dy4	8	2	2	3	1	–
8–9	Ln1	8	–	2	3	2	1
	Ln2	8	–	2	3	2	1
	Ln3	8	2	2	3	1	–
	Ln4	8	2	2	3	1	–

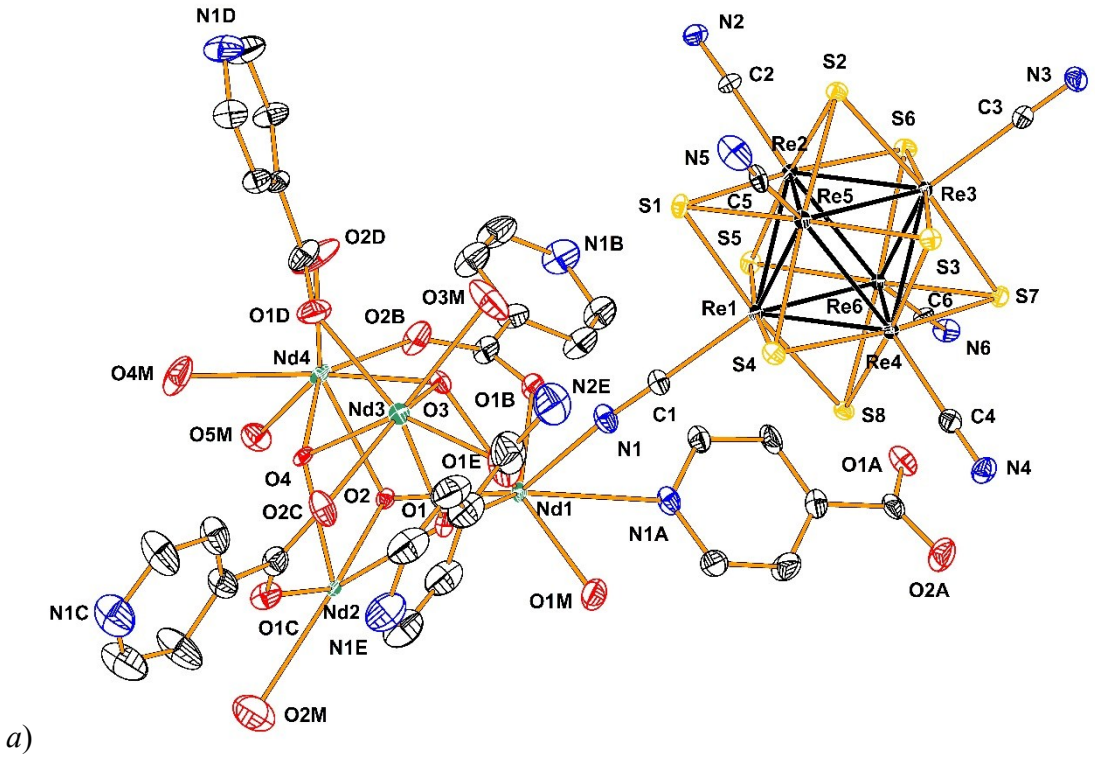

a)

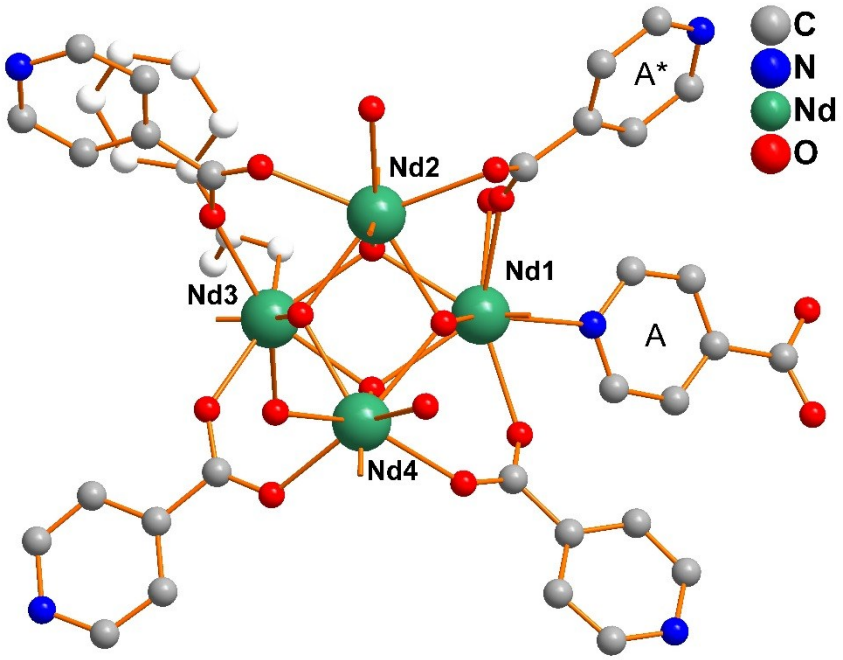

b)

Figure S1. Asymmetric unit of the structure **2** with atom represented by thermal ellipsoids drawn at 50% probability (*a*); $\{Nd_4(\mu_3\text{-}OH)_4(\mu\text{-ina})(ina)_3(H_2O)_{5.5}(C_6H_6N_2O)_{0.5}\}^{4+}$ building unit. Asterisk denotes symmetry-generated bridging *ina* ligand, symmetry code: -*x*+0.5; *y*-0.5; -*z*+1.5. Broken-off bonds mark the Nd–N_{CN} bonds (*b*). Hydrogen atoms are omitted for clarity.

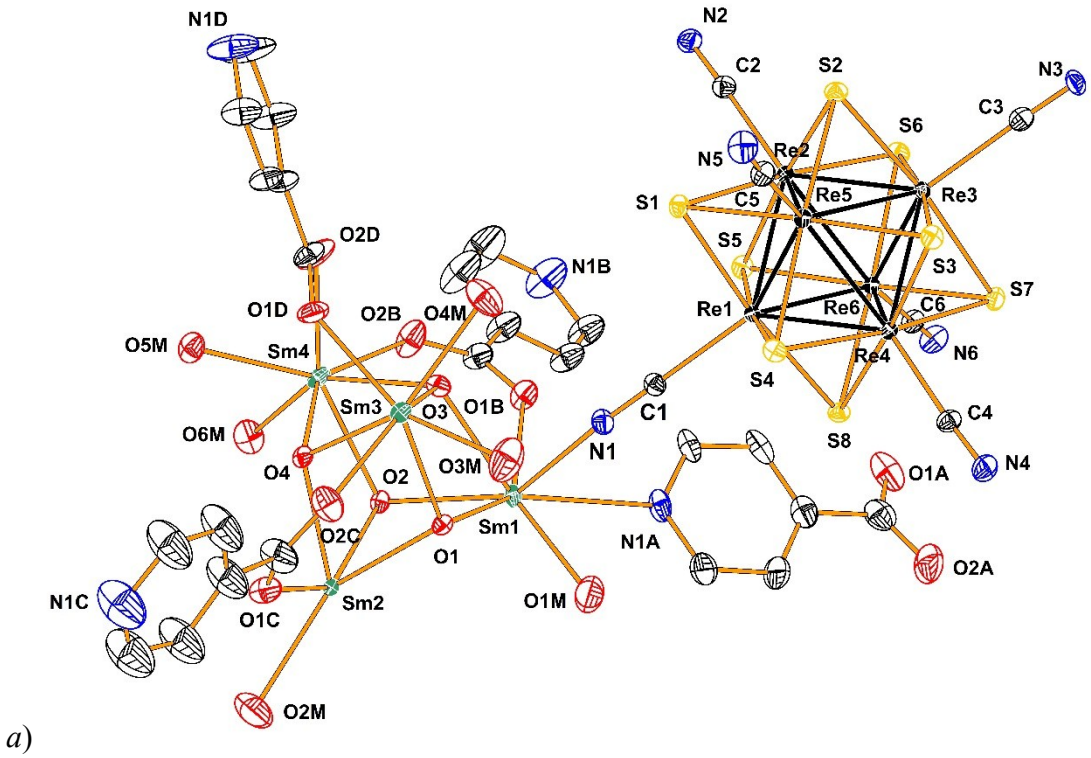

a)

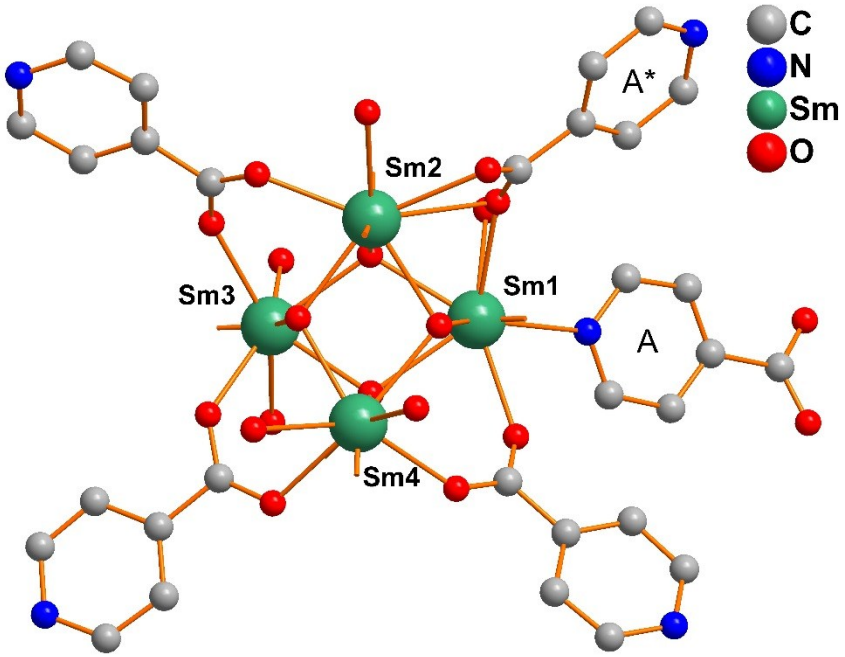

b)

Figure S2. Asymmetric unit of the structure **3** with atom represented by thermal ellipsoids drawn at 40% probability (*a*); $\{Sm_4(\mu_3\text{-}OH)_4(\mu\text{-ina})(ina)_3(H_2O)_6\}^{4+}$ building unit. Asterisk denotes symmetry-generated bridging *ina* ligand, symmetry code: -*x*+0.5; *y*-0.5; -*z*+1.5. Broken-off bonds mark the Sm–N_{CN} bonds (*b*). Hydrogen atoms are omitted for clarity.

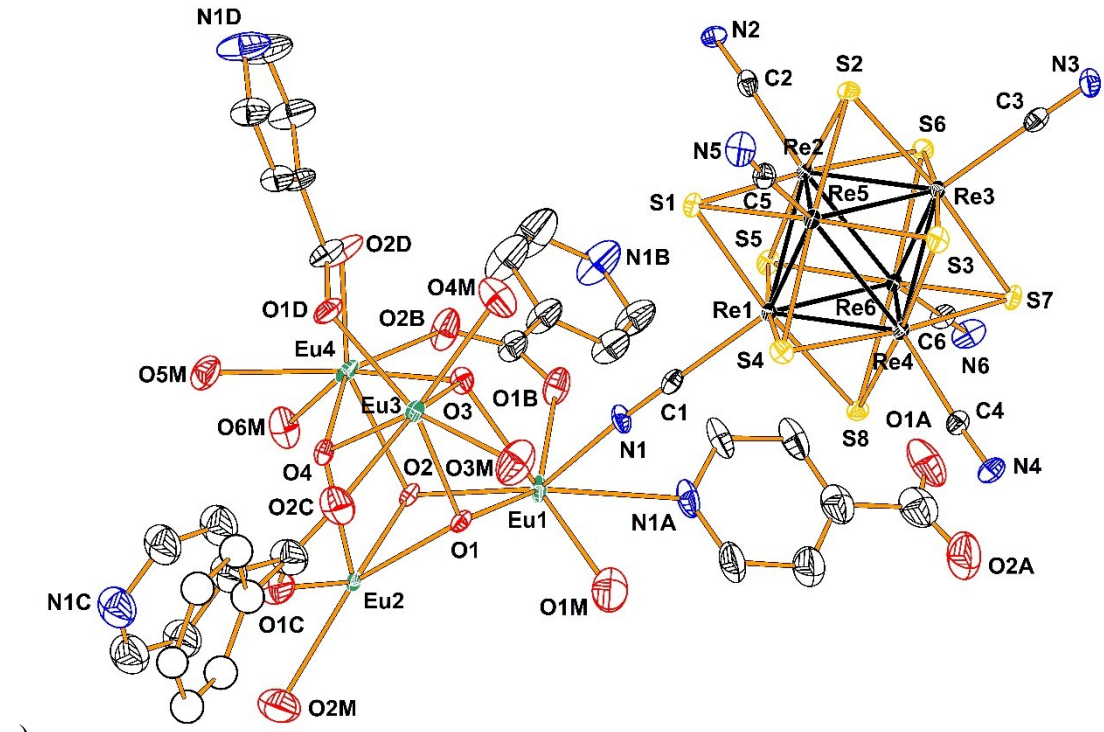

a)

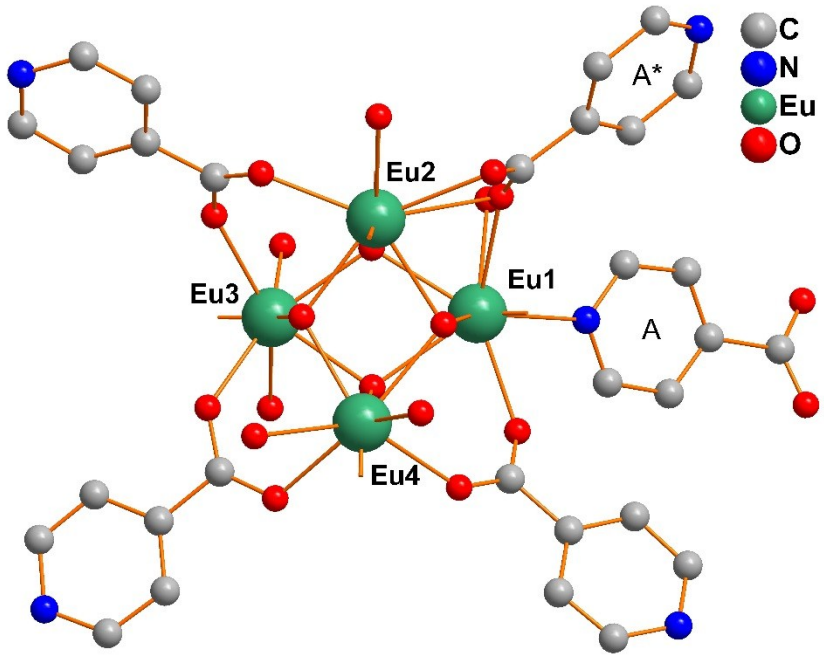

b)

Figure S3. Asymmetric unit of the structure **4** with atom represented by thermal ellipsoids drawn at 50% probability. Alternative position of disordered terminal *ina* ligand is shown as colorless balls (*a*); $\{Eu_4(\mu_3\text{-}OH)_4(\mu\text{-ina})(ina)_3(H_2O)_6\}^{4+}$ building unit. Asterisk denotes symmetry-generated bridging *ina* ligand, symmetry code: -*x*+0.5; *y*-0.5; -*z*+1.5. Broken-off bonds mark the Eu–N_{CN} bonds (*b*). Hydrogen atoms are omitted for clarity.

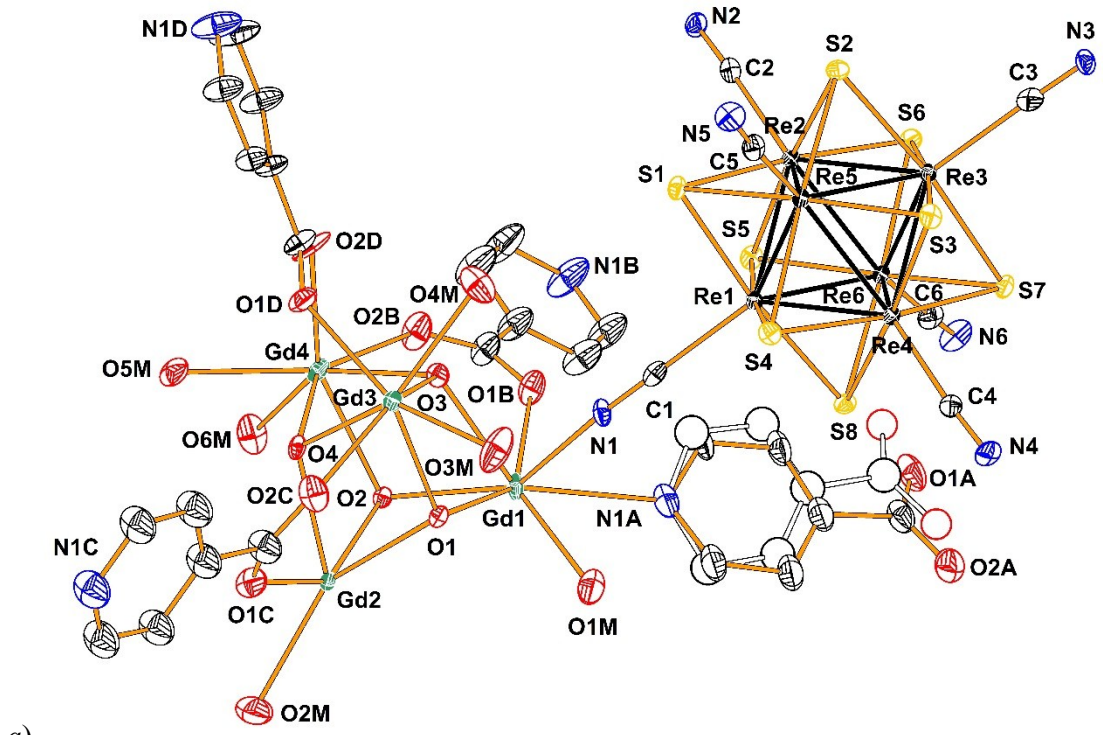

a)

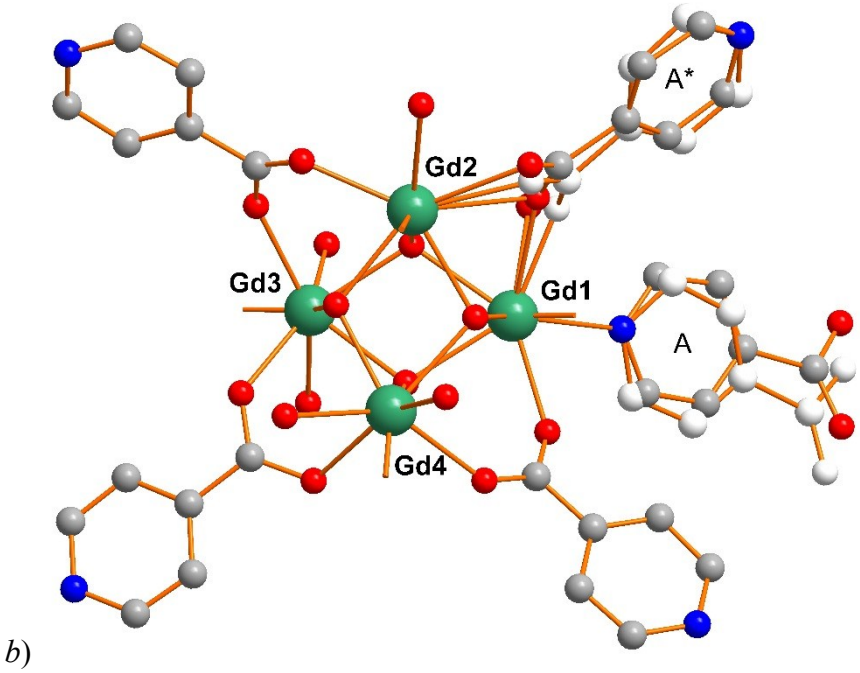

b)

Figure S4. Asymmetric unit of the structure **5** with atom represented by thermal ellipsoids drawn at 40% probability (*a*); $\{Gd_4(\mu_3\text{-}OH)_4(\mu\text{-ina})(ina)_3(H_2O)_6\}^{4+}$ building unit. Asterisk denotes symmetry-generated bridging *ina* ligand, symmetry code: -*x*+0.5; *y*-0.5; -*z*+1.5. Broken-off bonds mark the Gd–N_{CN} bonds (*b*). Alternative position of disordered bridging *ina* ligand is shown as colorless balls. Hydrogen atoms are omitted for clarity.

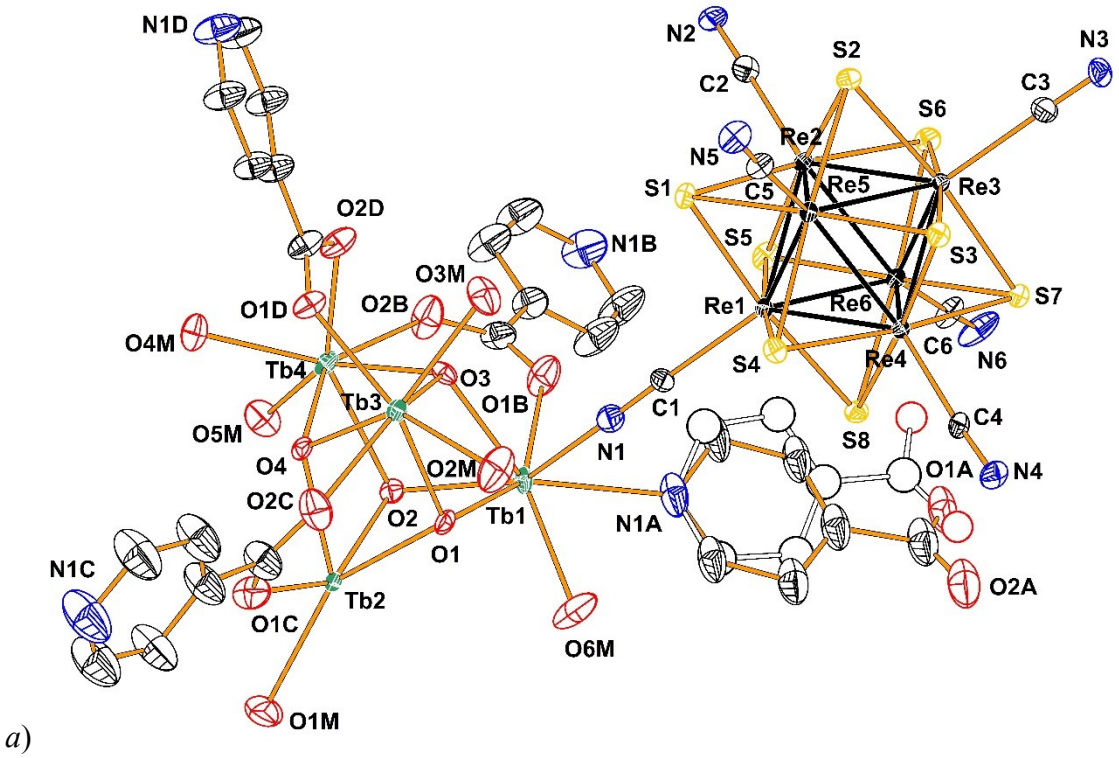

a)

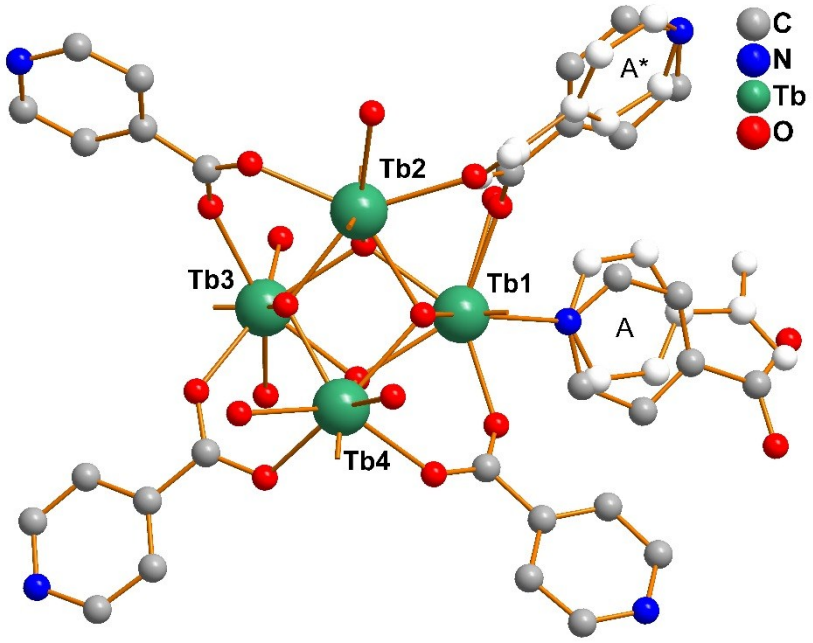

b)

Figure S5. Asymmetric unit of the structure **6** with atom represented by thermal ellipsoids drawn at 50% probability (*a*); $\{Tb_4(\mu_3\text{-}OH)_4(\mu\text{-ina})(ina)_3(H_2O)_5\}^{4+}$ building unit. Asterisk denotes symmetry-generated bridging *ina* ligand, symmetry code: -*x*+0.5; *y*-0.5; -*z*+1.5. Broken-off bonds mark the Tb–N_{CN} bonds (*b*). Alternative position of disordered bridging *ina* ligand is shown as colorless balls. Hydrogen atoms are omitted for clarity.

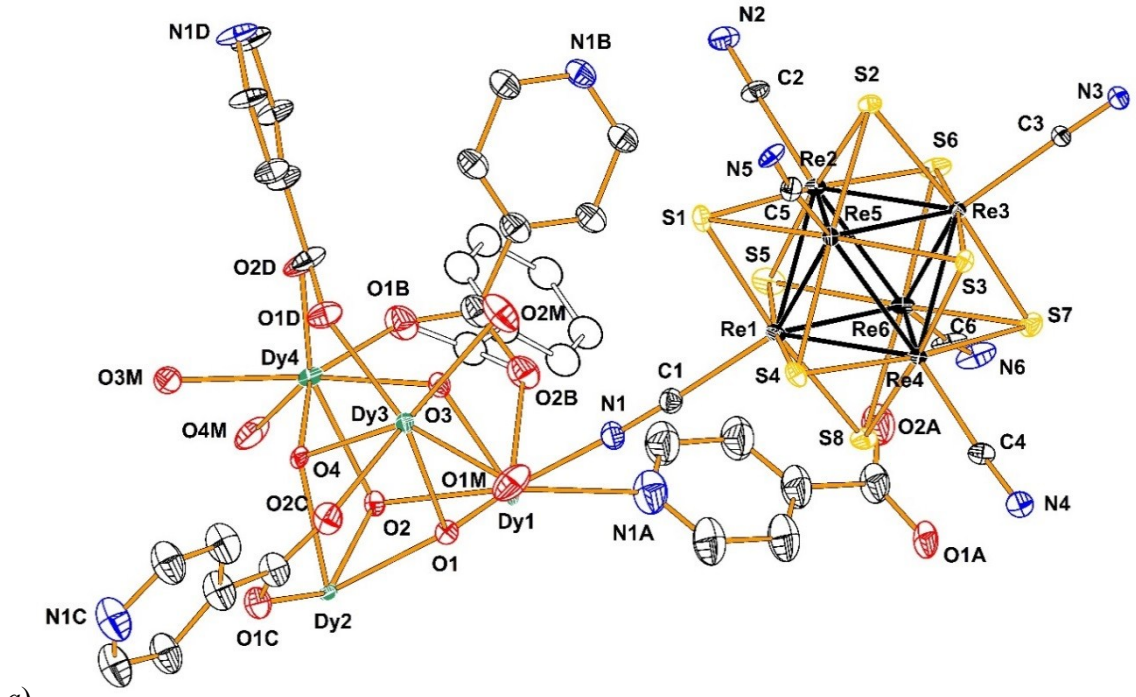

a)

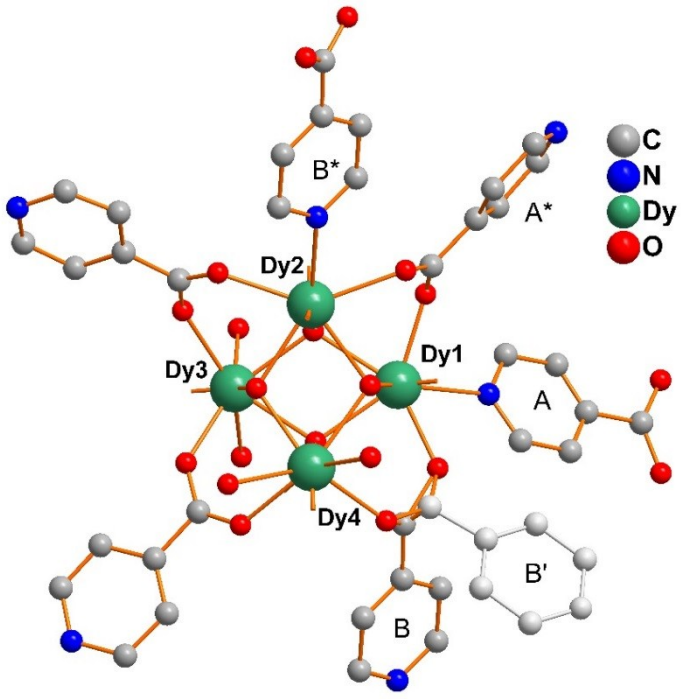

b)

Figure S6. Asymmetric unit of the structure **7** with atom represented by thermal ellipsoids drawn at 50% probability (*a*); $\{Dy_4(\mu_3\text{-}OH)_4(\mu\text{-}ina)_{1.6}(ina)_{2.4}(H_2O)_4\}^{4+}$ building unit. B and B′ denote the alternative positions of disordered *ina* ligand. Asterisks denote symmetry-generated bridging *ina* ligands. Symmetry codes: -*x*+0.5; *y*-0.5; -*z*+1.5 for A* and *x*; *y*-1; *z* for B*. Broken-off bonds mark the Dy–N_{CN} bonds (*b*). Alternative position of disordered bridging *ina* ligand is shown as colorless balls. Hydrogen atoms are omitted for clarity.

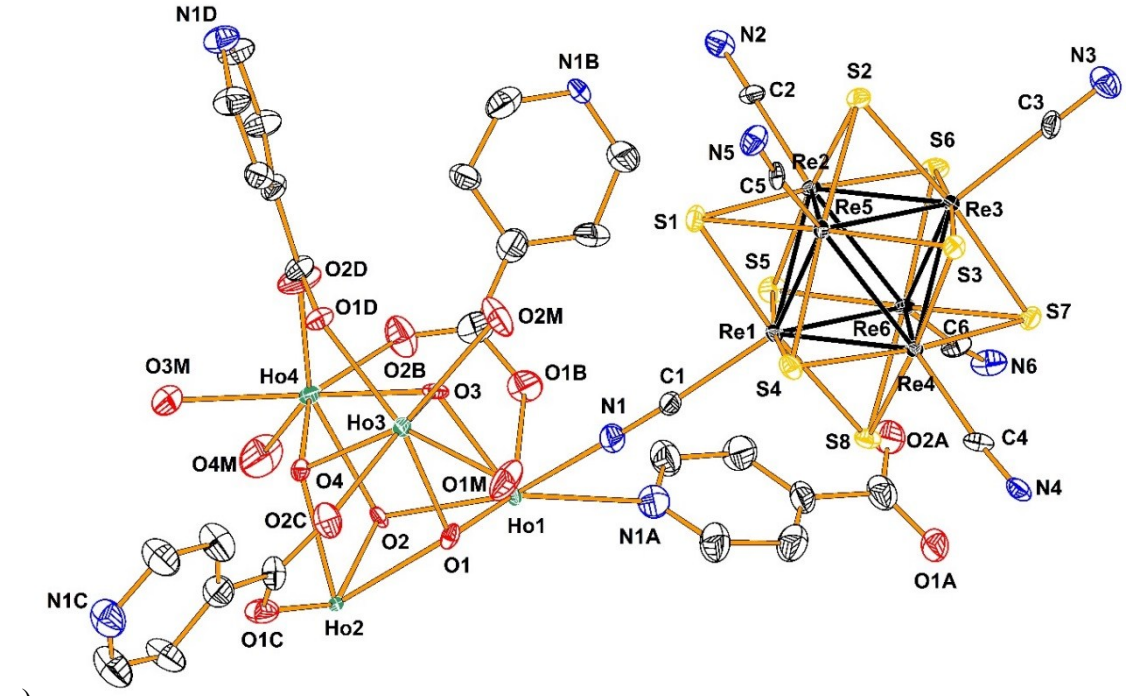

a)

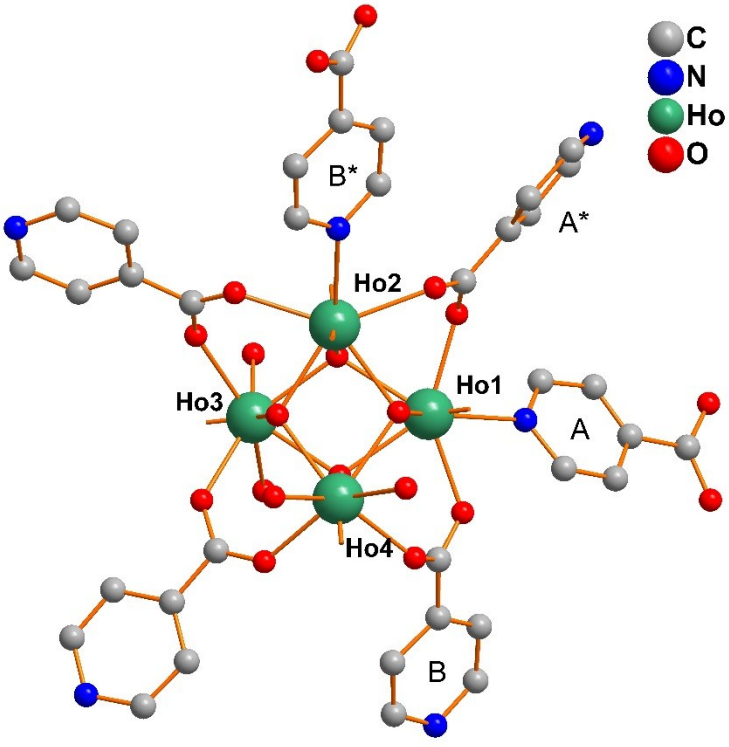

b)

Figure S7. Asymmetric unit of the structure **8** with atom represented by thermal ellipsoids drawn at 50% probability (*a*); $\{Ho_4(\mu_3\text{-}OH)_4(\mu\text{-}ina)_2(ina)_2(H_2O)_4\}^{4+}$ building unit. Asterisks denote symmetry-generated bridging *ina* ligands. Symmetry codes: -*x*+0.5; *y*-0.5; -*z*+1.5 for A* and *x*; *y*-1; *z* for B*. Broken-off bonds mark the Ho–N_{CN} bonds (*b*). Hydrogen atoms are omitted for clarity.

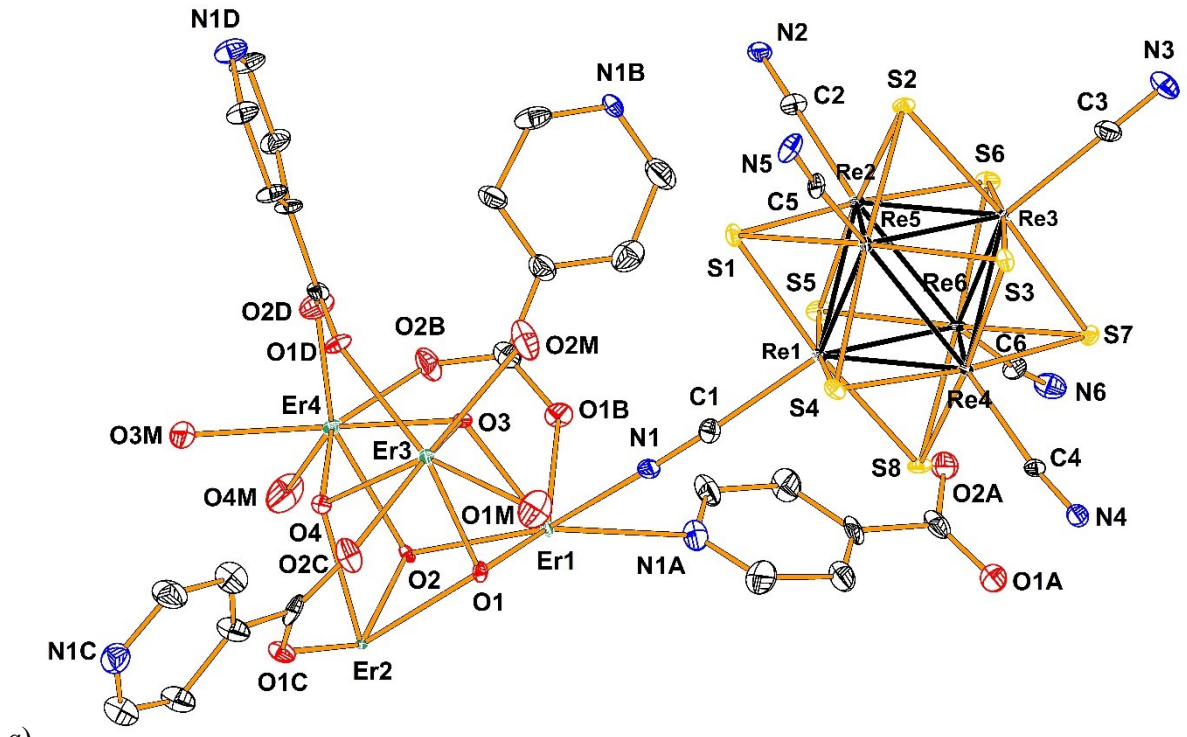

a)

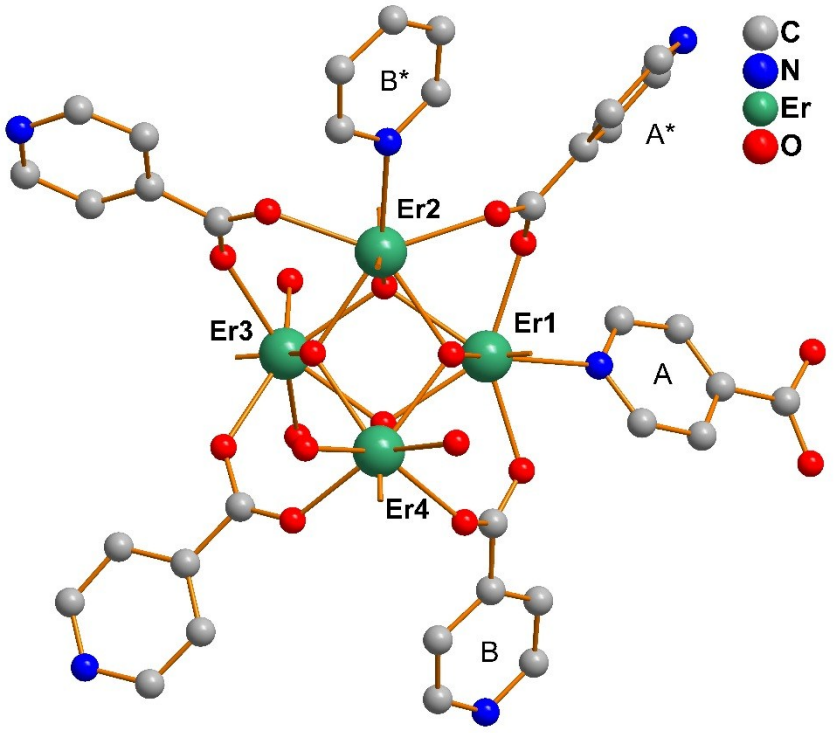

b)

Figure S8. Asymmetric unit of the structure **9** with atom represented by thermal ellipsoids drawn at 50% probability (*a*); $\{Er_4(\mu_3\text{-}OH)_4(\mu\text{-}ina)_2(ina)_2(H_2O)_4\}^{4+}$ building unit. Asterisks denote symmetry-generated bridging *ina* ligands. Symmetry codes: -*x*+0.5; *y*-0.5; -*z*+1.5 for A* and *x*; *y*-1; *z* for B*. Broken-off bonds mark the Er–N_{CN} bonds (*b*). Hydrogen atoms are omitted for clarity.

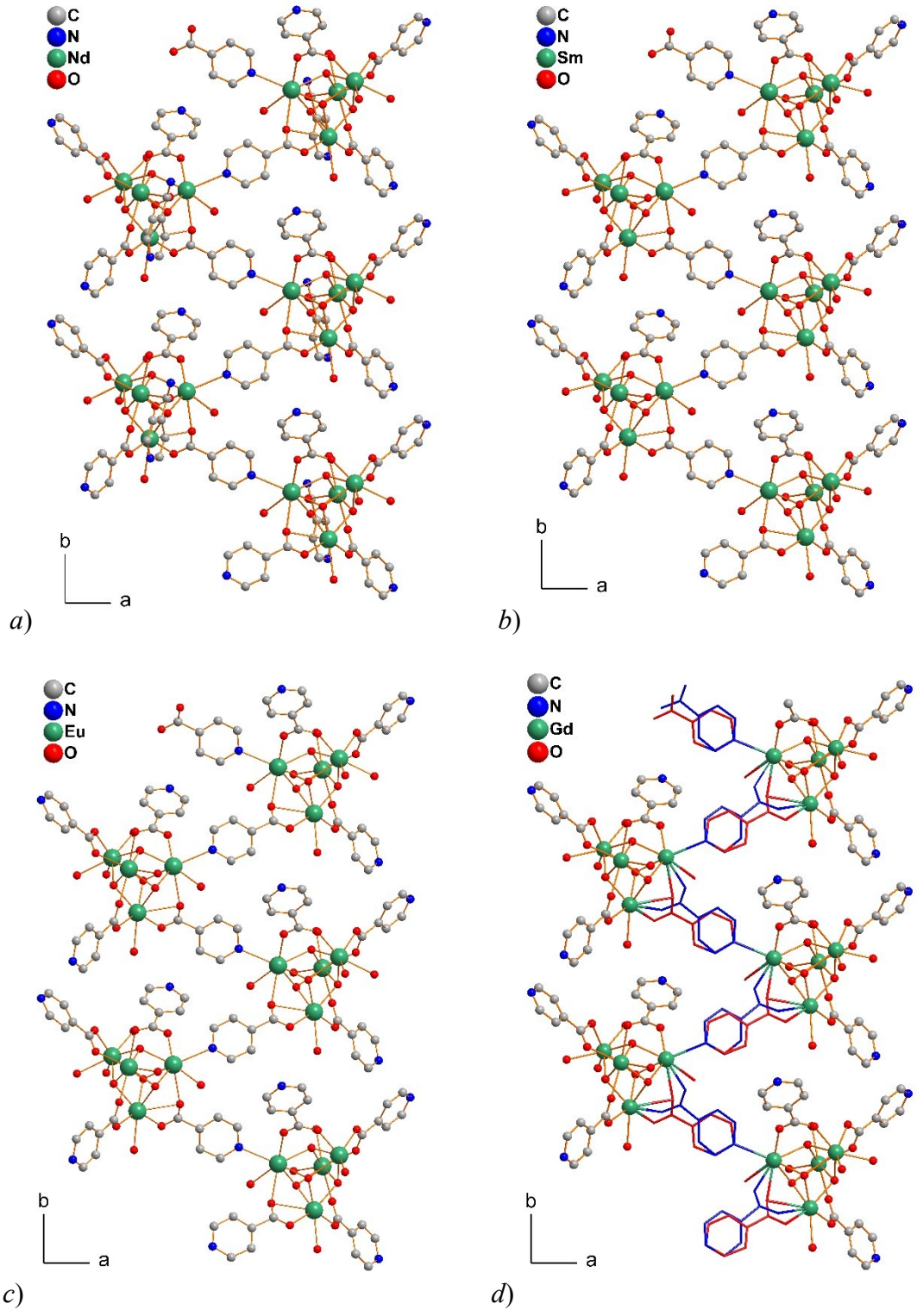

Figure S9. Structure of polymeric chains $\{Ln_4(\mu_3\text{-}OH)_4(\mu\text{-}ina)(ina)_3(H_2O)_6\}_n^{4n+}$ (Ln = Nd, Sm, Eu, Gd) in the structure of compounds **2**–**5** (*a*-*d*, respectively). Alternative positions of disordered linkers are drawn as blue and red sticks.

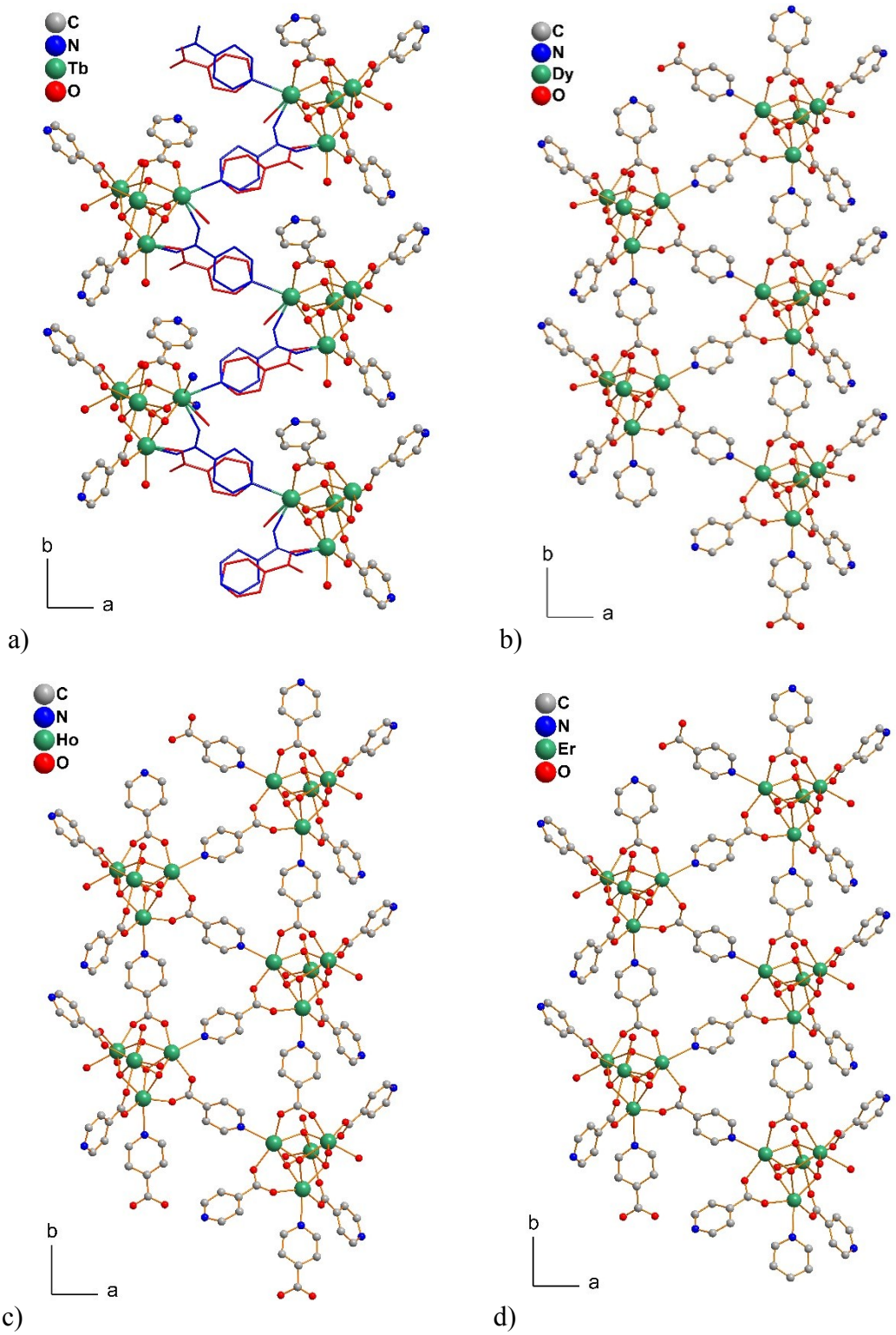

Figure S10. Structure of polymeric chains $\{Tb_4(\mu_3\text{-}OH)_4(\mu\text{-}ina)(ina)_3(H_2O)_5\}_n^{4n+}$ and $\{Ln_4(\mu_3\text{-}OH)_4(\mu\text{-}ina)_2(ina)_2(H_2O)_4\}_n^{4n+}$ (Ln = Dy, Ho, Er) in the structure of compounds **6–9** (*a*-*d*, respectively). Alternative positions of disordered linkers are drawn as blue and red sticks.

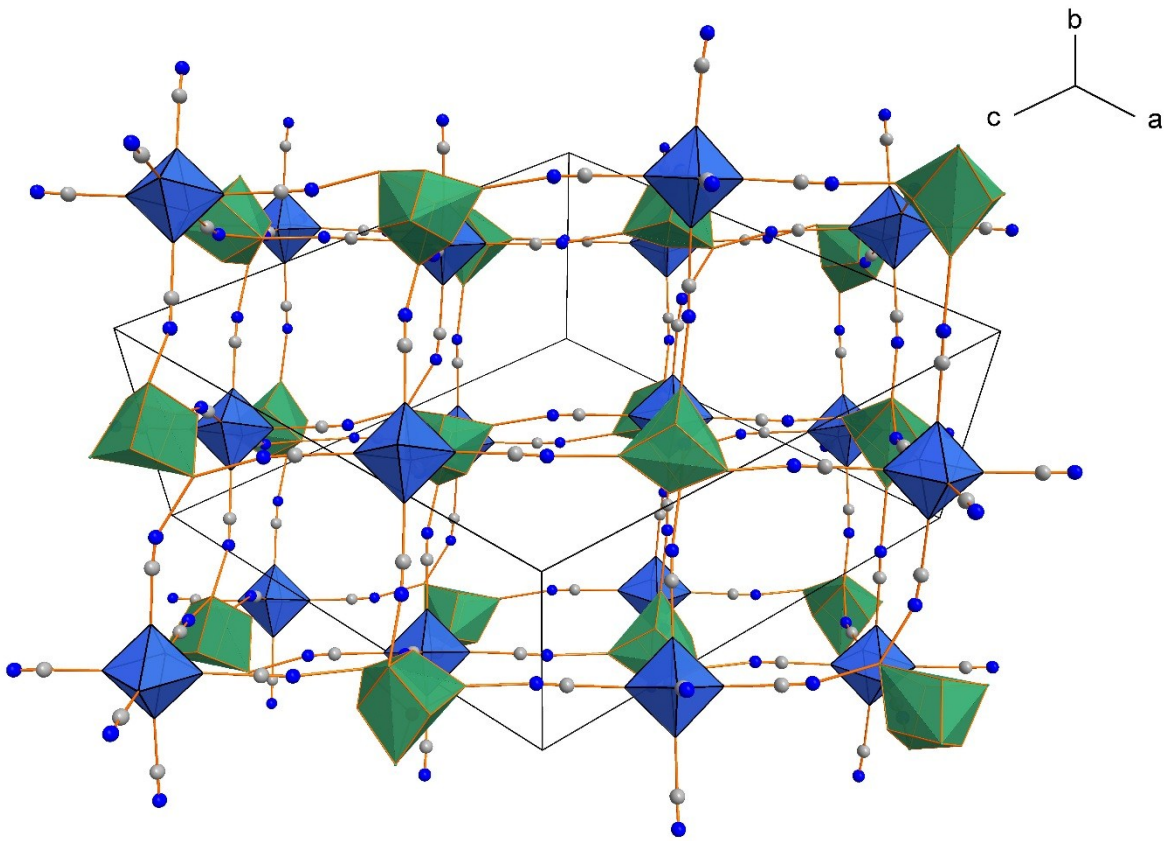

Figure S11. Polyhedral representation of the packing of $\{Pr_4(\mu_3\text{-}OH)_4\}^{8+}$ (green polyhedra) and $\{Re_6S_8\}^{2+}$ (blue polyhedra) cluster units in the structure **1**. The *ina* ions, μ_3-Se ligands and H_2O molecules are not shown.

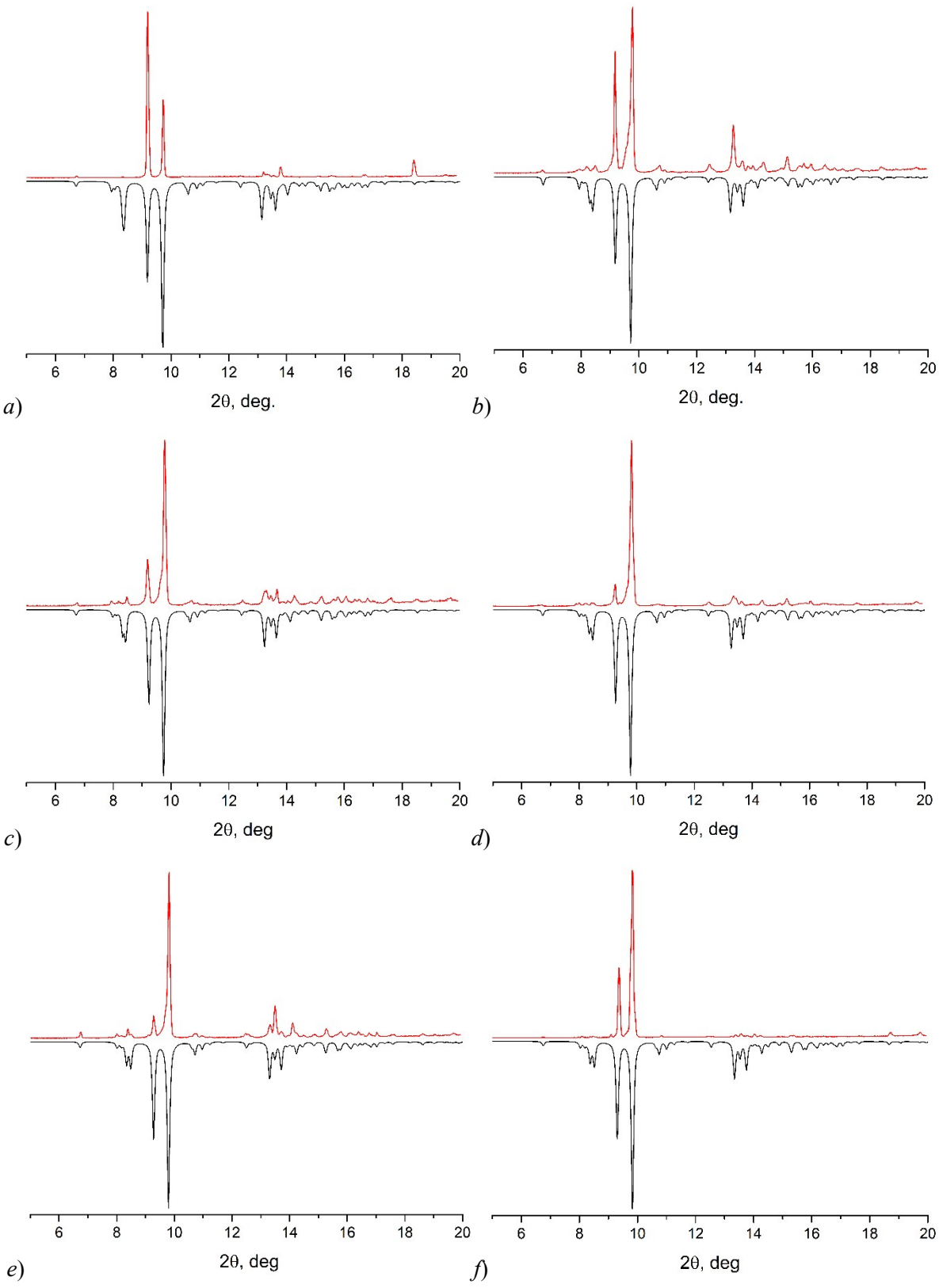
6 8 10 12 14 16 18 20
2θ, deg.
a)
b)
c)
d)
e)
f)

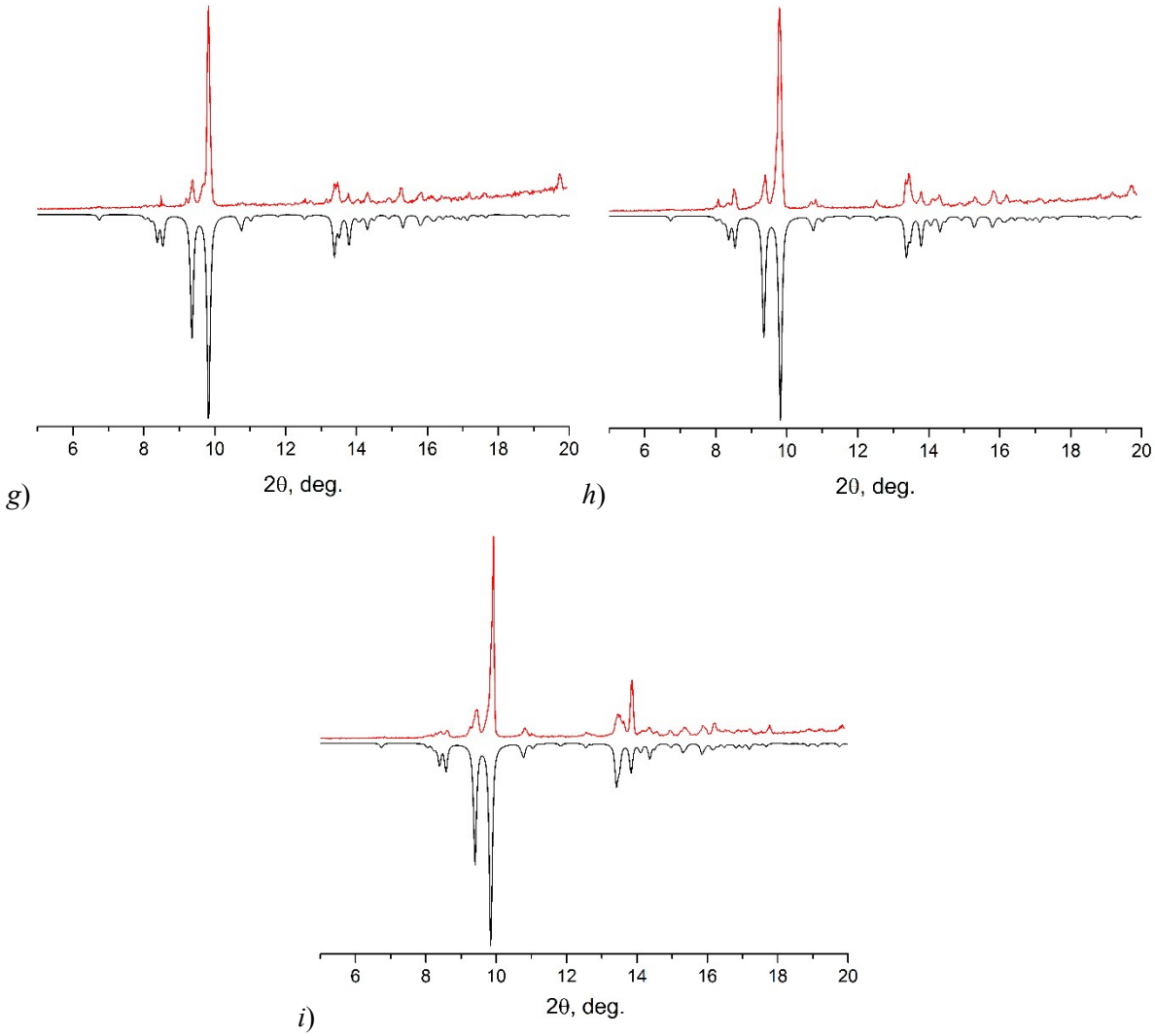

Figure S12. Experimental (red line) *vs* calculated (black line) powder X-Ray diffraction (PXRD) patterns of compounds **1**–**9** (*a*–*i*, respectively).

Table S3. Thermal mass loss of compounds **1–9** according to the TGA data.

	Range 1, °C	Mass loss 1	Range 2, °C	Mass loss 2	Total loss, amu / H_2O
1 (Ln = Pr)	25–150	5.0% = 143 amu	150–250	1.8% = 51 amu	194 / 10.8
2 (Ln = Nd)	25–146	4.4% = 127 amu	146–253	1.6% = 46 amu	173 / 9.6
3 (Ln = Sm)	25–146	3.3% = 96 amu	146–265	2.2% = 64 amu	160 / 8.9
4 (Ln = Eu)	25–161	5.5% = 159 amu	161–245	1.7% = 49 amu	208 / 11.6
5 (Ln = Gd)	25–162	3.5% = 102 amu	146–270	1.7% = 50 amu	152 / 8.4
6 (Ln = Tb)	25–152	4.1% = 119 amu	152–240	1.6% = 46 amu	165 / 9.2
7 (Ln = Dy)	25–160	4.2% = 124 amu	160–238	1.4% = 41 amu	165 / 9.2
8 (Ln = Ho)	25–150	4.5% = 132 amu	150–274	1.5% = 44 amu	176 / 9.8
9 (Ln = Er)	25–150	4.0% = 118 amu	150–258	1.7% = 50 amu	168 / 9.3

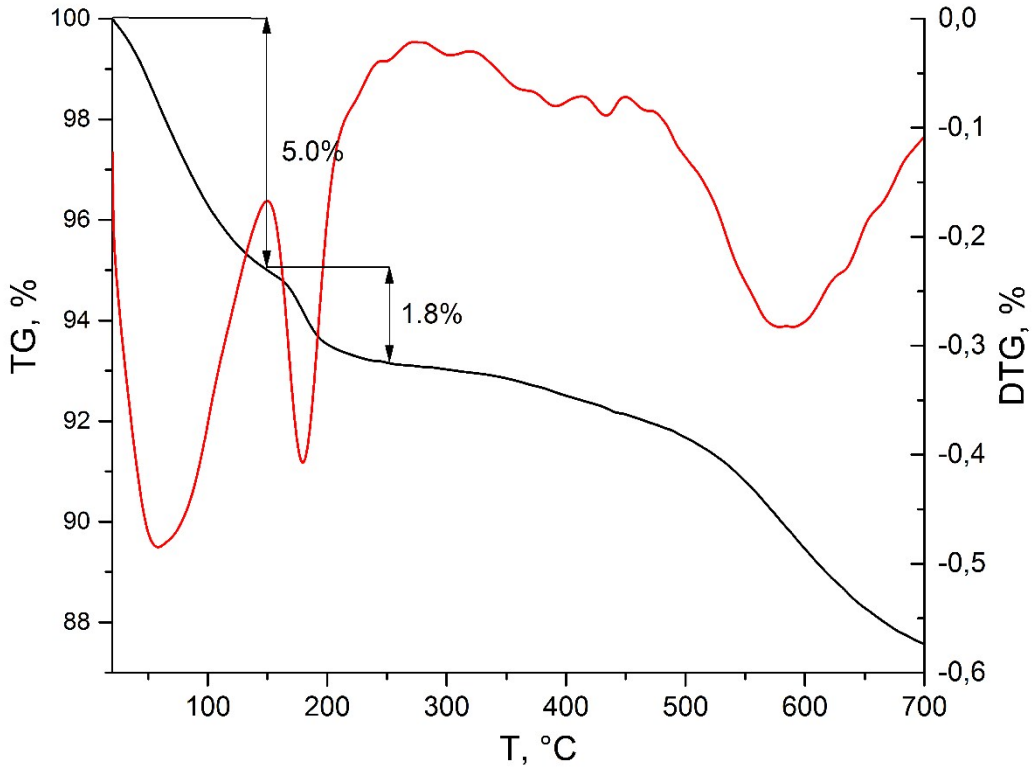

Figure S13. TG (black line) and DTG (red line) curve of compound **1**.

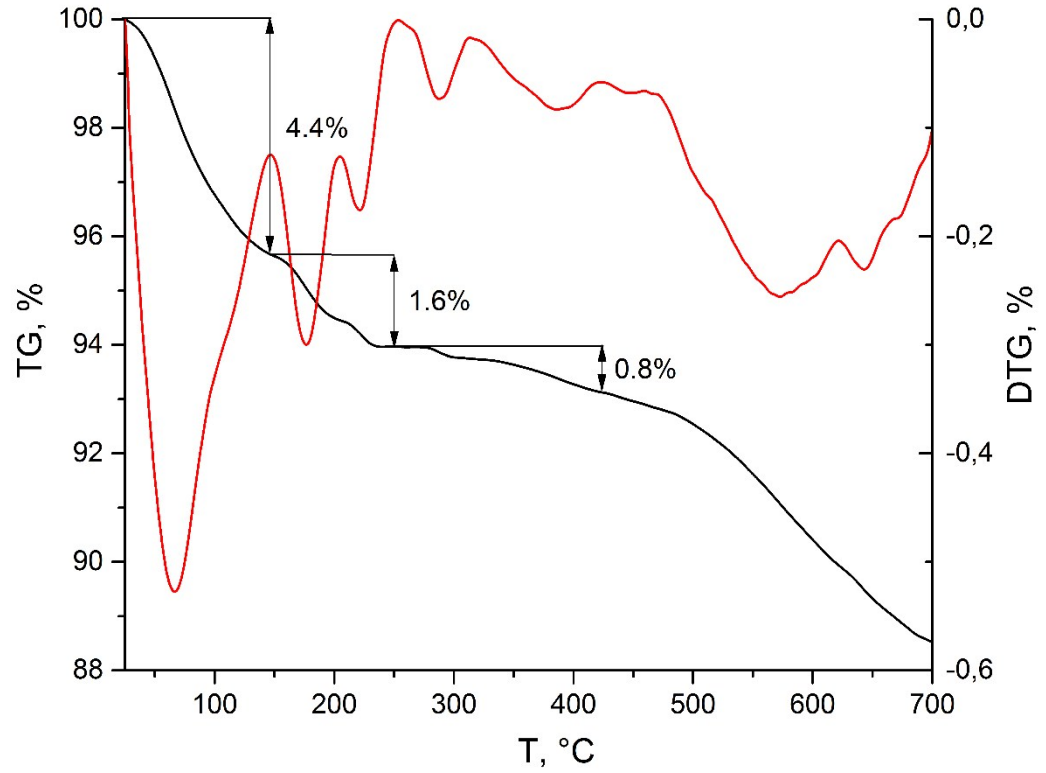

a)

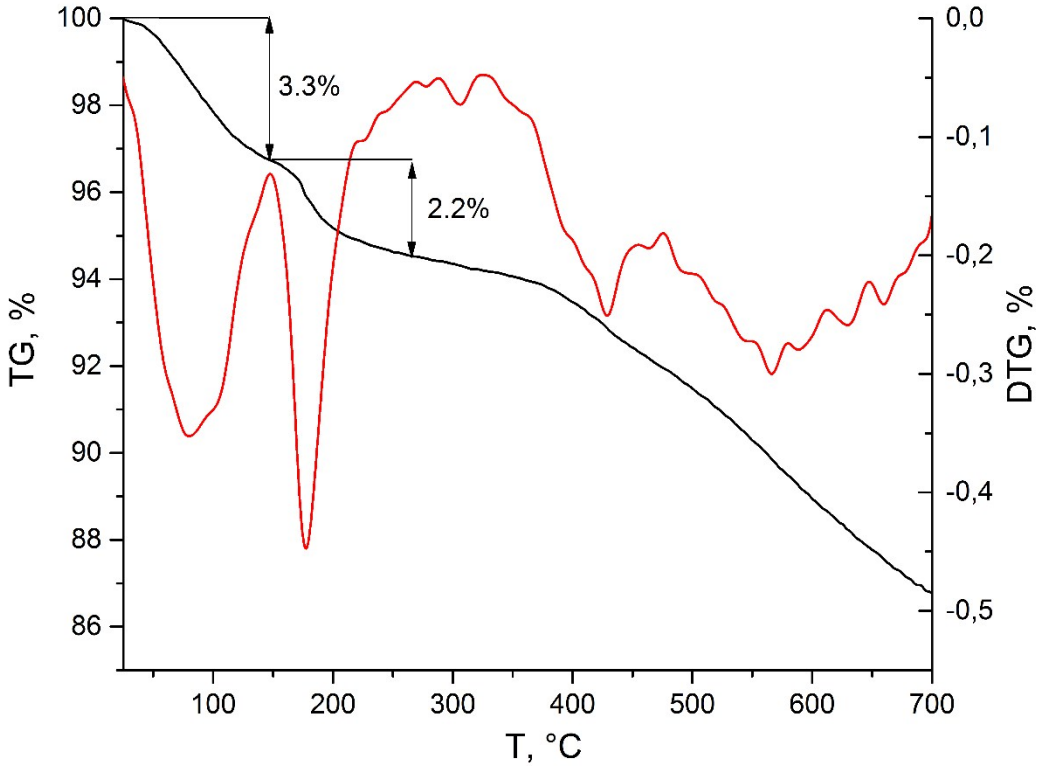

b)

Figure S14. TG (black line) and DTG (red line) curves of compounds **2** (*a*) and **3** (*b*).

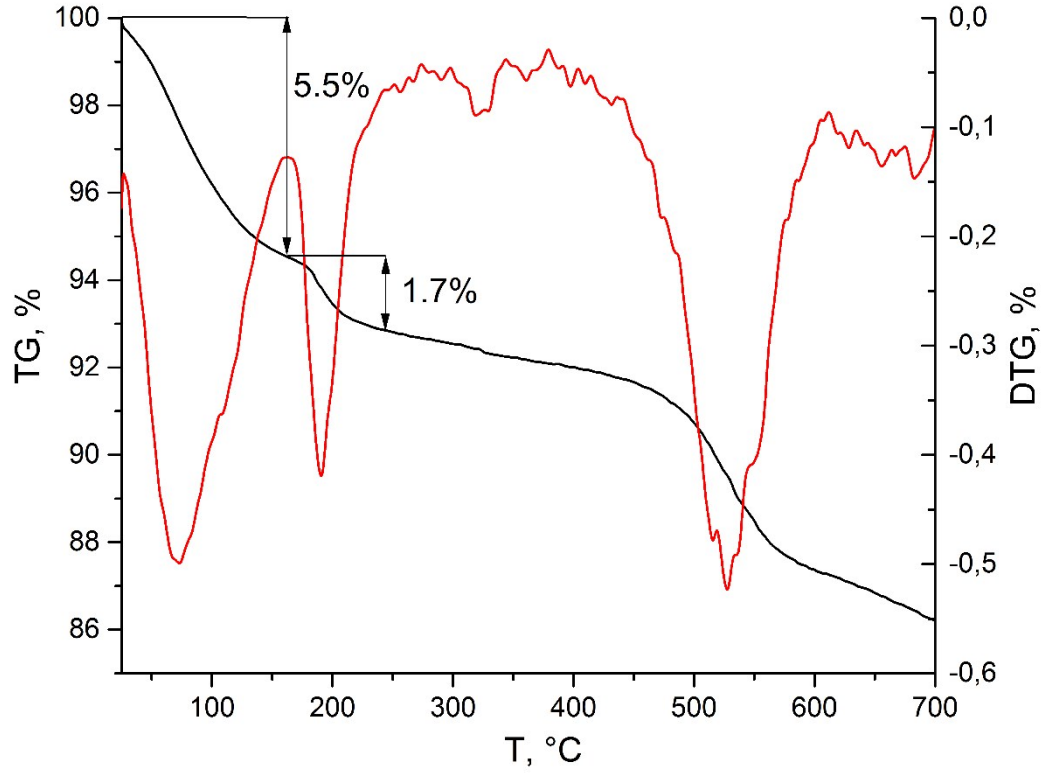

a)

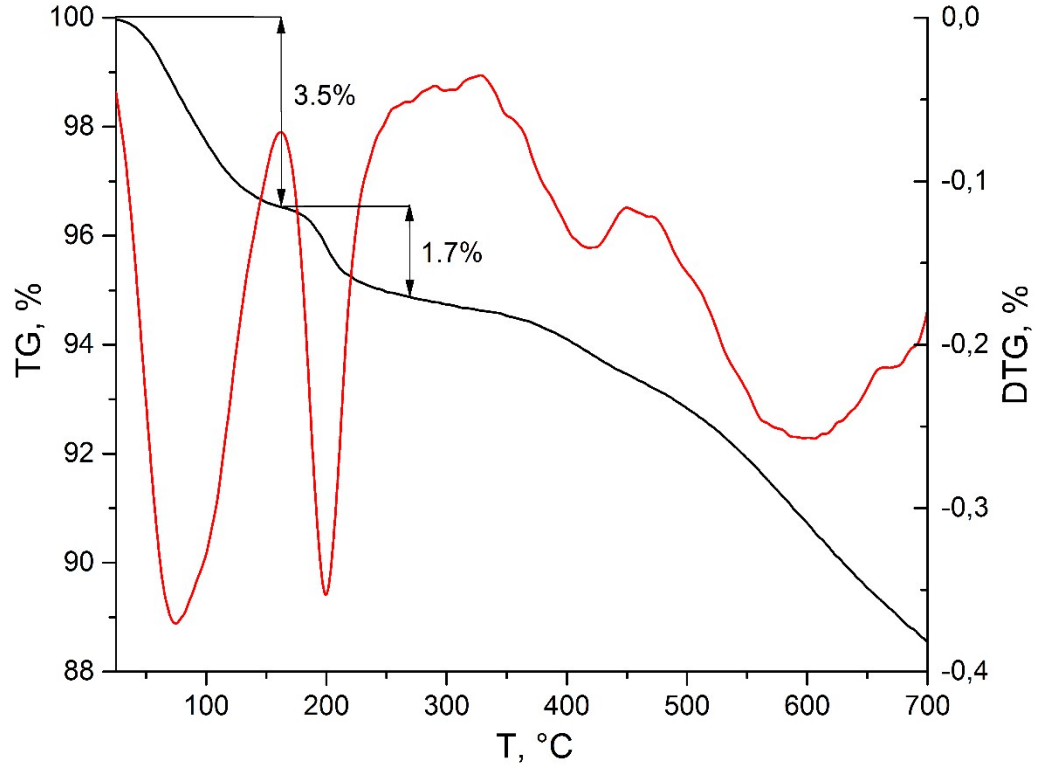

b)

Figure S15. TG (black line) and DTG (red line) curves of compounds **4** (*a*) and **5** (*b*).

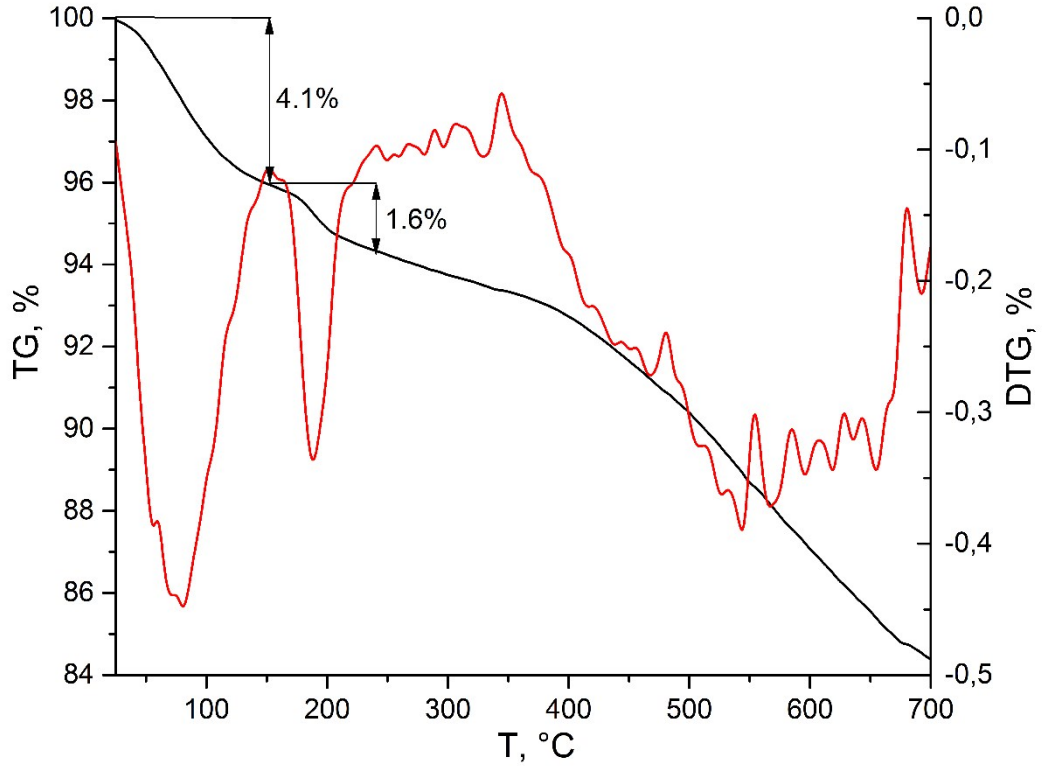

a)

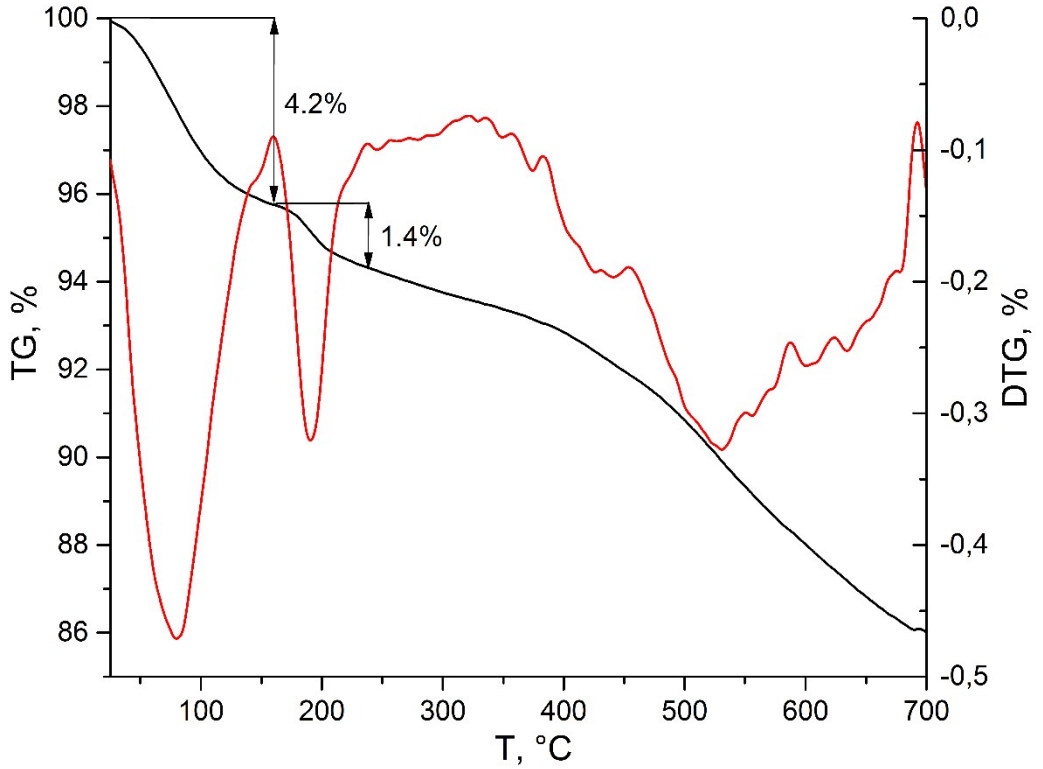

b)

Figure S16. TG (black line) and DTG (red line) curves of compounds **6** (*a*) and **7** (*b*).

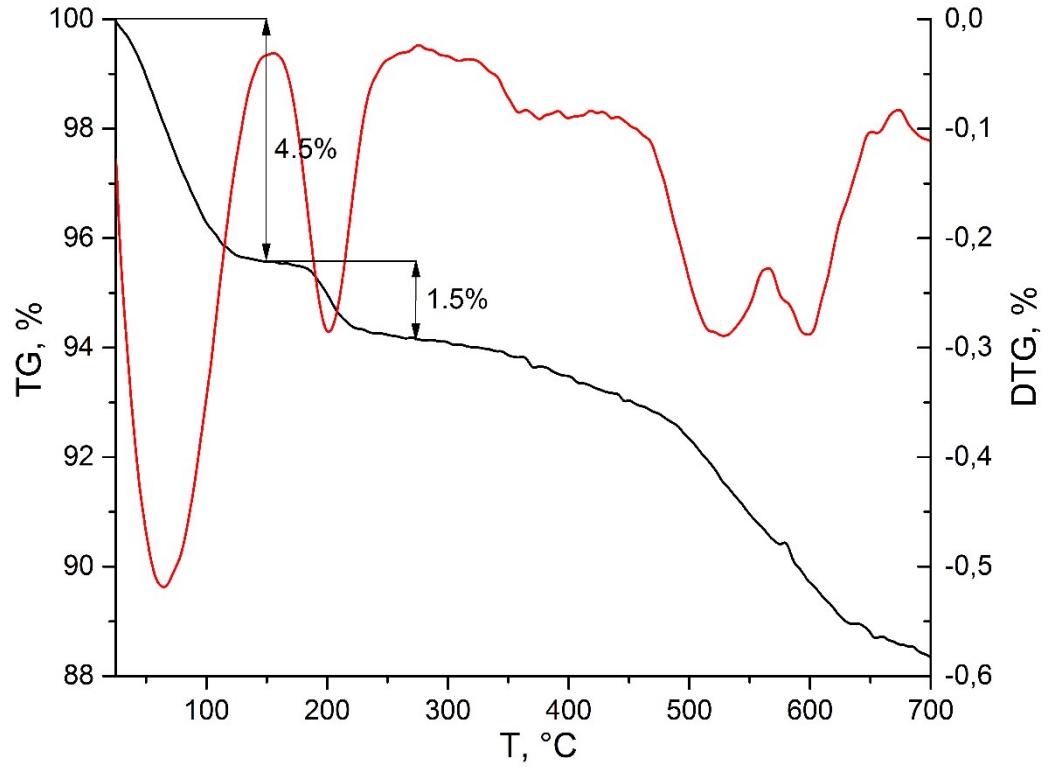

a)

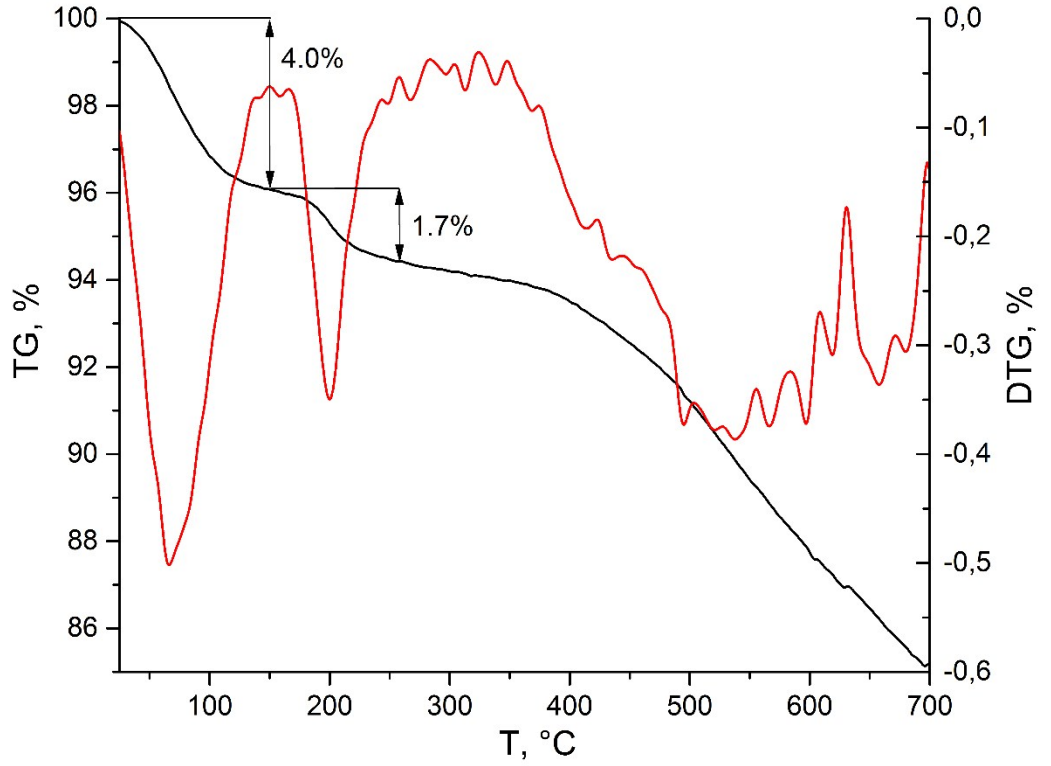

b)

Figure S17. TG (black line) and DTG (red line) curves of compounds **8** (*a*) and **9** (*b*).

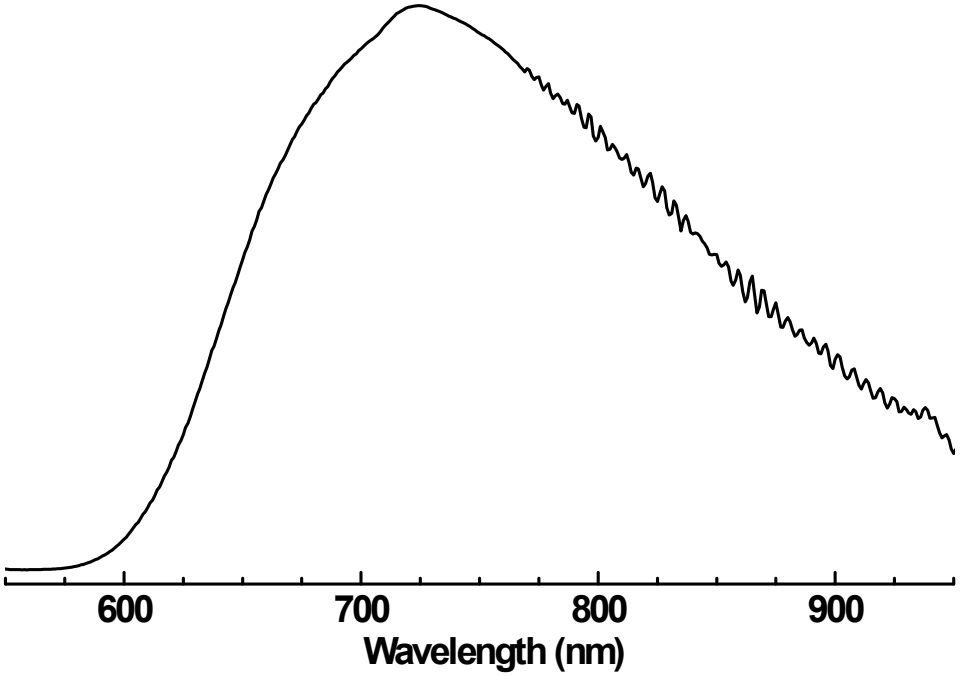

Figure S18. Emission spectrum of the crystalline sample of compound **6** upon excitation by 355 nm laser.

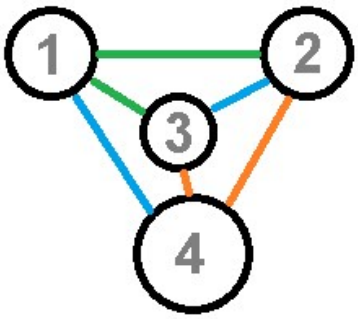

Figure S19. Exchange interaction pathways assumed in model B in the least-squares fit of the magnetic dc data of **5**; Δ(2–4) and Δ(3–4) represent the shortest, Δ(1–3) and Δ(1–2) the medium, and Δ(1–4) and Δ(2–3) the largest distances between the four Gd^{3+} ions.

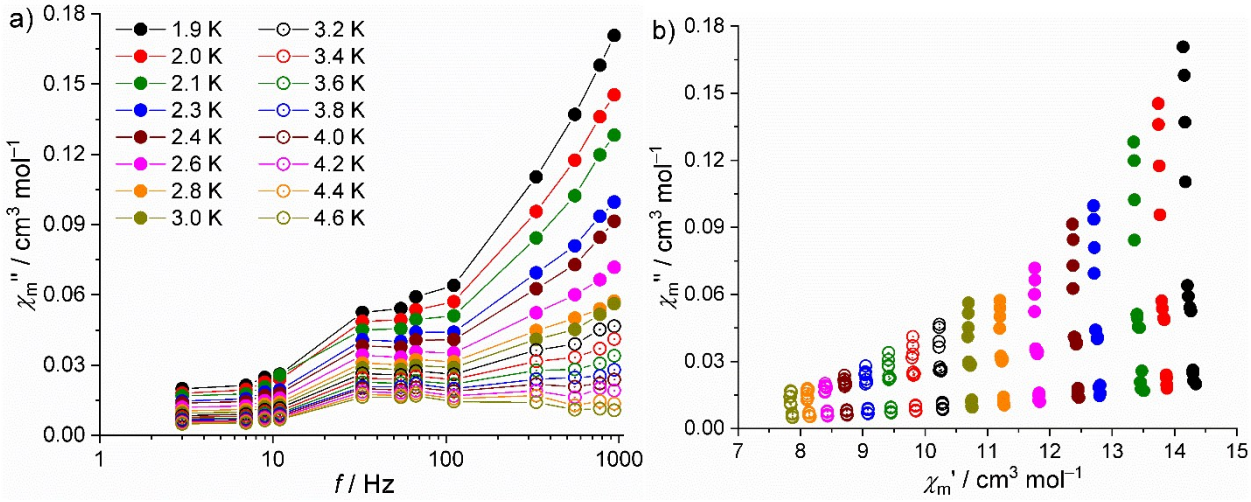

Figure S20. Magnetic ac data of **7** at zero static bias field: a) out-of-phase molar susceptibility χ_m'' vs. frequency f (lines are guides for the eyes); b) out-of-phase χ_m'' vs. in-phase molar susceptibility χ_m' (symbol/color codes in a) for both plots).

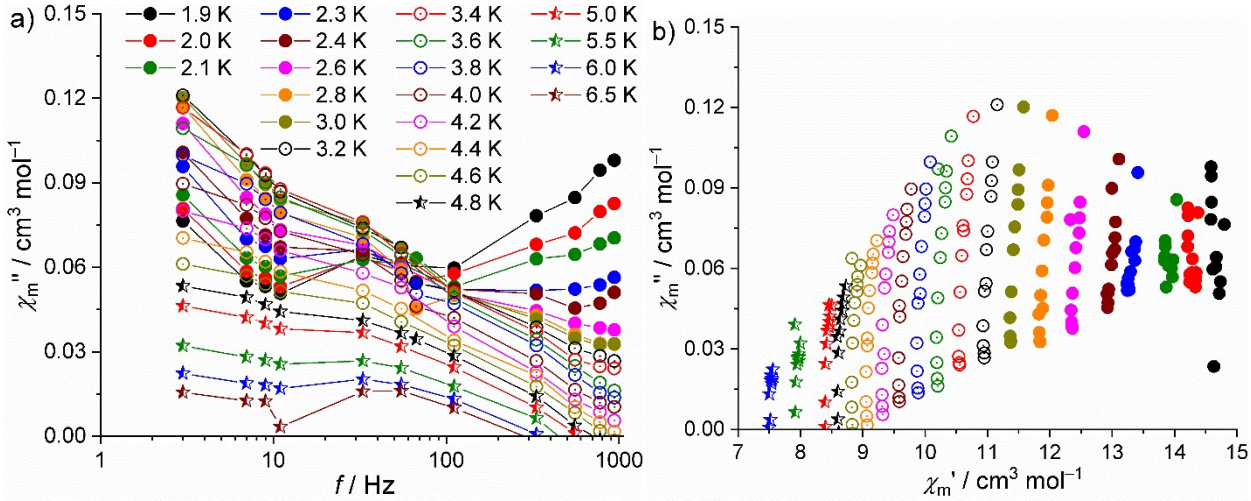

Figure S21. Magnetic ac data of **7** at 0.1 T static bias field: a) out-of-phase molar susceptibility χ_m'' vs. frequency f (lines are guides for the eyes); b) out-of-phase χ_m'' vs. in-phase molar susceptibility χ_m' (symbol/color codes in a) for both plots).